Letter

Visual Feedback Disturbance Rejection Control for an Amphibious Bionic Stingray Under Actuator Saturation

Haiyan Cheng, Bin Fang, Qing Liu, Jinhua Zhang, and Jun Hong

Dear Editor,

This letter is concerned with visual feedback disturbance rejection control for an amphibious bionic stingray subject to actuator saturation with internal and external disturbances. A visual feedback control method is designed for a dynamic nonlinear system on yaw angle of the amphibious bionic stingray via a finite-time extended-state-observer, which is proved to achieve finite-time stability via a Lyapunov method. Finally, simulation results verify the effectiveness on the visual feedback control method.

With the development of science and technology, various unmanned equipment are widely used and developed in military, civil and other fields [1]. Many underwater or surface unmanned vehicles are developed to show important application prospects in marine monitoring, logistics support, marine agriculture, [2] and [3], etc. Many researchers draw inspiration from natural biological fish for developing variety of bionic autonomous surface or underwater vehicles, such as bionic tuna [4], bionic manta ray [5], etc. We also designed and produced an amphibious bionic stingray in [6] based on fluid-structure interaction simulation results. Like most surface or underwater vehicles, realizations of expectation control in complex and uncertain dynamic environment is an important premise for its practical applications [7].

To realize precise control of controlled plant, disturbance-rejection control methods are adopted by many researchers to deal with uncertain dynamic environment or imprecise system model [8]. Among the existing disturbance-rejection control methods, extended-state-observer-based control is one to estimating both total disturbances and unknown system states with the least information on the controlled plant [9]. Extended-state-observer is proposed by Han [10], which is successfully applied in bionic caudal fin [11], autonomous surface vehicle [12] and so on. A major difference between these control methods is that different proofs and designs for extended-state-observers. Furthermore, collection, feedback and processing of visual information provides a convenient way to realize some autonomous motion controls for bionic autonomous surface or underwater vehicles [13]. Moreover, actuator saturation is an important consideration in robot control system [14]. Therefore, it is interesting and challenging to design an appropriate method for realizing visual feedback control using extended-state-observer for the designed amphibious bionic stingray subject to actuator saturation.

Corresponding author: Jinhua Zhang.

Citation: H. Y. Cheng, B. Fang, Q. Liu, J. H. Zhang, and J. Hong, "Visual feedback disturbance rejection control for an amphibious bionic stingray under actuator saturation," *IEEE/CAA J. Autom. Sinica*, vol. 10, no. 2, pp. 566–568, Feb. 2023.

H. Y. Cheng, B. Fang, J. H. Zhang, and J. Hong are with the Key Laboratory of Education Ministry for Modern Design and Rotor-Bearing System, Xi'an Jiaotong University, Xi'an 710049, China (e-mail: chenghaiyan8023@163.com; binfang@mail.xjtu.edu.cn; jjshua@mail.xjtu.edu.cn; jhong@mail.xjtu.edu.cn)..

Q. Liu is with the School of Automation and Information Engineering, Xi'an University of Technology, Xi'an 710048, China (e-mail: 948481478@qq.com).

Color versions of one or more of the figures in this paper are available online at http://ieeexplore.ieee.org.

Digital Object Identifier 10.1109/JAS.2023.123237

Consider above descriptions, this letter mainly focuses on modeling, control method design, stability analysis and simulation verification for the amphibious bionic stingray. The main contribution of this letter are outlined as: 1) An amphibious bionic stingray is introduced and a dynamic system on yaw angle is established. 2) A finite-time extended-state-observer proved by Lyapunov method is designed to estimate total disturbances in the dynamic system. 3) Controller integrated error feedback and disturbance rejection compensation is designed and analyzed under actuator saturation restriction.

Bionic stingray modeling: According to biological observations and fluid-structure interaction simulation studies, an amphibious bionic stingray is designed and fabricated in [6], which is shown in Fig. 1 with main structural components. Through the innovative design of screw-type drive shafts, array-type fin surfaces can realize undulating bionic motion on stingray under driving actions of micro motors. Using the visual module integrated in the amphibious bionic stingray front-end, visual feedback motion control can be achieved by communication and control module.

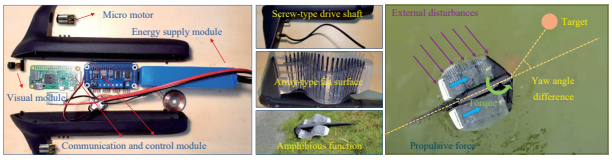

Fig. 1. Amphibious bionic stingray with main structural components.

The amphibious bionic stingray can be used as surface or underwater vehicles by different balance of gravity and buoyancy. Rectilinear and rotary motions can be realized by adjusting speed and steering of two micro motors. It is worth noting that athletic abilities of the amphibious bionic stingray is limited by its actuator, it takes 2.8 s for the amphibious bionic stingray to complete 90° rotation. Moreover, tracking control schematic diagram is depicted in Fig. 1 for yaw angle between a specific target and the amphibious bionic stingray. In this letter, only tracking control of yaw angle is considered temporarily for the amphibious bionic stingray, which is expressed as the following dynamic model:

$$\dot{\theta}(t)=\omega(t),\quad m_\theta\dot{\omega}(t)=T_u(t)+T_n(t)+T_d(t) \tag{1}$$

where m_θ is the mass containing hydrodynamic mass, $\theta(t)$ is the yaw angle, $\omega(t)$ is the yaw angular speed, $T_n(t)$ is used to indicate unmodeled dynamics, $T_d(t)$ represents the external disturbances, $T_u(t)$ is the control input which can be adjusted by speed difference of two micro motors for the amphibious bionic stingray. Letting $T_u/m_\theta=gu(t)$, where $u(t)$ is the voltage signal difference between two driving motors, which realizes different motor speeds to achieve yaw motion for the amphibious bionic stingray, g is the gain on $u(t)$. Then, the dynamic model (1) is further written as below:

$$\dot{\theta}(t)=\omega(t),\quad \dot{\omega}(t)=T_o(t)+\hat{g}u_m\text{sat}(u(t)) \tag{2}$$

where $\hat{g}$ is the adjustable parameter as a gain estimate value, u_m is the positive saturation limit of $u(t)$, $\text{sat}(u(t))=\text{sign}(u(t))\min\{|u(t)|/u_m,1\}$, $T_o(t)=\tilde{g}u(t)+(T_n(t)+T_d(t))/m_\theta$ represents the total disturbances with $\tilde{g}=g-\hat{g}$. It is worth mentioning that the total disturbances usually is considered derivative bounded in extended-state-observer-based control methods [10]–[12]. Therefore, $T_o(t)<\Delta_1$ is satisfied with Δ_1 is a positive constant.

Control method: A schematic diagram is shown in Fig. 2 for the control method proposed in this letter, which is mainly composed of a yaw angle image recognition algorithm, a finite-time extended-state-observer and a error feedback controller under actuator saturation. Using the visual module shown in Fig. 1, the yaw angle can be obtained for the amphibious bionic stingray by digital image processing technology, and its solution process is displayed in Algorithm 1.

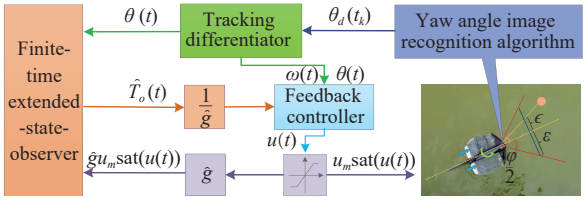

Fig. 2. Schematic diagram on visual feedback control method.

Algorithm 1 Yaw Angle Image Recognition Algorithm

1: Image frame capture of video streaming, image denoising and conversion to $YCbCr$ color space.
2: Image binarization process using predetermined thresholds.
3: Morphological operations on erosion, dilation and hole filling.
4: Connected region extraction, center of gravity determination.
5: Calculate yaw angle $\theta_d(t_k)$ using center of gravity coordinates.

As shown in the yaw angle calculation diagram in Fig. 2, $\theta_d(t_k)$ is the yaw angle calculated from image frame

$$\theta_d(t_k) = \arctan\left(\frac{\tan(\varphi/2)\epsilon}{\varepsilon}\right) \tag{3}$$

where ϵ is the distance between the center of gravity on target and the center in the current image frame, ε is the half length of image frame, φ the fixed viewing angle of the visual module. Considering the lack of image, calculation time and other problems during image recognition, the value of $\theta_d(t_k)$ cannot be obtained continuously or has a longer time interval. By a tracking differentiator designed in [10], a continuous yaw angle tracking trajectory can be obtained as

$$\bar{\omega}(t) = \dot{\bar{\theta}}(t) = f_{\text{han}}(\bar{\theta}(t) - \theta_d(t_k), \bar{\theta}(t), \gamma_v, \gamma_f) \tag{4}$$

where $\bar{\theta}(t)$ is the tracking trajectory of $\theta_d(t_k)$, the expression on $f_{\text{han}}(\cdot)$ is introduced in [10], the differential signal of $\bar{\theta}(t)$ is expressed as $\bar{\omega}(t)$, γ_v and γ_f are velocity regulation factor and filter regulation factor, respectively. In this letter, $\bar{\theta}(t)$ calculated by the tracking differentiator (4) is regard as the yaw angle $\theta(t)$ in the dynamical system (2). To estimate the total disturbances in the dynamical system (2), a finite-time extended-state-observer is designed as follows:

$$\begin{cases} \dot{\hat{\theta}}(t) = \hat{\omega}(t) - \alpha_1 f_1(t) \\ \dot{\hat{\omega}}(t) = \hat{T}_o(t) - \alpha_2 f_2(t) + \hat{g} u_m \text{sat}(u(t)) \\ \dot{\hat{T}}_o(t) = -\alpha_3 f_3(t) \end{cases} \tag{5}$$

where α_1, α_2 and α_3 are adjustable positive parameters, $f_1(t)$, $f_2(t)$ and $f_3(t)$ are functions concerning observation errors, $\hat{\theta}(t)$, $\hat{\omega}(t)$ and $\hat{T}_o(t)$ are observed values of $\theta(t)$, $\omega(t)$ and $T_o(t)$, respectively. An observation error system is obtained by the finite-time extended-state-observer (5) and the dynamical system (2) as below:

$$\begin{cases} \dot{e}_\theta(t) = e_\omega(t) - \alpha_1 f_1(t) \\ \dot{e}_\omega(t) = e_T(t) - \alpha_2 f_2(t) \\ \dot{e}_T(t) = -\alpha_3 f_3(t) - \dot{T}_o(t) \end{cases} \tag{6}$$

where $e_\theta(t) = \hat{\theta}(t) - \theta(t)$, $e_\omega(t) = \hat{\omega}(t) - \omega(t)$ and $e_T(t) = \hat{T}_o(t) - T_o(t)$. Using a finite-time convergent differentiator designed in [15], $e_\omega(t) = \dot{e}_\theta(t) + \alpha_1 f_1(t)$ and $e_T(t) = \alpha_2 f_2(t) + \alpha_1 \dot{f}_1(t) + \ddot{e}_\theta(t)$ can be obtained by calculating $\dot{e}_\theta(t)$ and $\ddot{e}_\theta(t)$. Then, functions $f_i(t)$ with $i = 1,2,3$ are designed as $f_1(t) = e_\theta(t) + |e_\theta(t)|^\delta \text{sign}(e_\theta(t))$, $f_2(t) = e_\omega(t) + |e_\omega(t)|^\delta \text{sign}(e_\omega(t))$ and $f_3(t) = e_T(t) + |e_T(t)|^\delta \text{sign}(e_T(t)) + \text{sign}(e_T(t))$ with $0 < \delta < 1$. The observation error system (6) is further written as

$$\dot{E}(t) = AE(t) + B|E(t)|^\delta + C\dot{T}_o(t) - \alpha_3 C \text{sign}(e_T(t)) \tag{7}$$

where $B = \text{diag}\{\alpha_1 \text{sign}(e_\theta(t)), \alpha_2 \text{sign}(e_\omega(t)), \alpha_3 \text{sign}(e_T(t))\}$, $E(t) = \begin{bmatrix} e_\theta(t) \\ e_\omega(t) \\ e_T(t) \end{bmatrix}$, $A = \begin{bmatrix} -\alpha_1 & 1 & 0 \\ 0 & -\alpha_2 & 1 \\ 0 & 0 & -\alpha_3 \end{bmatrix}$, $C = \begin{bmatrix} 0 \\ 0 \\ 1 \end{bmatrix}$.

For yaw angle tracking control of the amphibious bionic stingray, both desired angle and angular velocity are 0, on basis of the finite-time extended-state-observer (5), a tracking error feedback controller is designed under actuator saturation as follows:

$$u(t) = u_0(t) - \hat{T}_o(t)\hat{g}^{-1}u_m^{-1} \tag{8}$$

where $u_0(t) = \hat{g}^{-1}(\beta_1\theta(t) + \beta_2\omega(t))$ with β_1, β_2 are two adjustable parameters, which can be expressed as $u_0(t) = \hat{g}^{-1}F_c\vartheta(t)$ with $F_c = [\beta_1 \ \beta_2]$ and $\vartheta(t) = [\theta(t) \ \omega(t)]^T$.

Stability analysis: Two theorems are derived to prove the stability of the dynamic systems (2) under the proposed control method of this letter. For obtaining stability results, a lemma is reviewed first.

Lemma 1 [16]: For a system $x_l(t) = G_l x_l(t) + J_l \text{sat}(F_l x_l(t))$ with $x(t) \in \mathbb{R}^{n\times 1}$ and $G_l + J_l F_l$ is Hurwitz. If $x_l(t) \in \Phi(H_l)$ with $\Phi(H_l) \triangleq \{x_l(t) : |H_l x_l(t)| \le 1\}$, then, one has that

$$\text{sat}(F_l x_l(t)) = \sum_{i=1}^{2} \eta_i(\sigma_i F_l + \bar{\sigma}_i H_l)x_l(t) \tag{9}$$

where σ_i and $\bar{\sigma}_i$ are elements of a sat $\{0,1\}$ with $\sigma_i + \bar{\sigma}_i = 1$, $0 \le \eta_i \le 1$ and $\sum_{i=1}^{2}\eta_i = 1$. There is a Lyapunov function $V_l(t) = x^T(t)Q_l x(t)$ with a positive-definite matrix Q_l, if $\dot{V}_l(t) < 0$ for all $x(t) \in \Theta(Q_l, \varrho_l)$ with an ellipsoid $\Theta(Q_l, \varrho_l) = \{x(t) : V_l(t) \le \varrho_l\}$, then the ellipsoid $\Theta(Q_l, \varrho_l)$ is a strictly invariant set.

Theorem 1: For the observation error system (7), if there are adjustable parameters $\alpha_1 > 0$, $\alpha_2 > 0$ and $\alpha_3 > \Delta_1$ in the finite-time extended-state-observer (5), then the observation error $E(t)$ converge to null matrix in finite-time.

Proof: A function satisfying the Lyapunov conditions is constructed for the observation error system (6) as follows:

$$V_e(t) = E^T(t)PE(t) \tag{10}$$

taking derivative of the Lyapunov function (10), one has that

$$\begin{aligned} \dot{V}_e(t) = {} & (\dot{T}_o(t) - \alpha_3 \text{sign}(e_T(t)))(C^T PE(t) + E^T(t)PC) \\ & + E^T(t)(A^T P + PA)E(t) \\ & + |E^T(t)|^\delta B^T PE(t) + E^T(t)PB|E(t)|^\delta. \end{aligned} \tag{11}$$

According to the expression A, there are appropriate parameters α_1, α_2 and α_3 to make the expression $A^T P + PA = -N$ hold on, with N is the positive definite matrix. Because $\dot{T}_o(t)$ is bounded, the parameter α_3 can be adjusted to $\alpha_3 > \dot{T}_o(t)$. Therefore, the derivative of $V_e(t)$ is further derived as

$$\begin{aligned} \dot{V}_e(t) &\le -E^T(t)NE(t) - 2\|DP^{\frac{1-\delta}{2}}\|\|E^T(t)\|^{\frac{1+\delta}{2}} P^{\frac{1+\delta}{2}}|E(t)|^{\frac{1+\delta}{2}} \\ &\le -2\|DP^{\frac{1-\delta}{2}}\|V_e^{\frac{1+\delta}{2}}(t), \end{aligned} \tag{12}$$

where $D = \text{diag}\{\alpha_1, \alpha_2, \alpha_3\}$. According to the finite-time stability theory as in [17], convergence time is satisfied with the following inequality for the finite-time extended-state-observer (5):

$$t_e \le V_e^{\frac{1-\delta}{2}}(t_0) / \left((1-\delta)\|DP^{\frac{1-\delta}{2}}\|\right) \tag{13}$$

where $V_e(t_0)$ represents the initial time of the function $V_e(t)$, which is related to the initial value of the observation errors. ■

Theorem 2: Consider the dynamic systems (2) under the tracking error feedback controller (8), for all $\vartheta(t) \in \Theta(Q_c, \varrho_c) \triangleq \{\vartheta(t) : \vartheta^T(t) \times Q_c\vartheta(t) \le \varrho_c\}$, if there is a row vector $H_c \in \mathbb{R}^{1\times 2}$ such that

$$(G_c + J_c S_c)^T Q_c + Q_c(G_c + J_c S_c) < 0 \tag{14}$$

$$\Theta(Q_c, \varrho_c) \subset \Phi(H_c) \triangleq \{\vartheta(t) : |H_c\vartheta(t)| \le 1 - \Delta_2\} \tag{15}$$

with $S_c = \sum_{i=1}^{2}\eta_i(\sigma_i F_c + \bar{\sigma}_i H_c)$, then the ellipsoid $\Theta(Q_c, \varrho_c)$ is a contractively invariant set with constant Δ_2 is satisfied with $1 > \Delta_2 > \Delta_1 u_m^{-1}\hat{g}^{-1}$, which requires $\hat{g} > \Delta_1 u_m^{-1}$ hold on.

Proof: When parameter $\hat{g}$ is satisfied with $\hat{g} > \Delta_1 u_m^{-1}$, the tracking error feedback controller (8) is derived as

$$\text{sat}(u(t)) = \overline{\text{sat}}(u_0(t)) - \hat{T}_o(t)u_m^{-1}\hat{g}^{-1} \tag{16}$$

where $\overline{\text{sat}}(u_0(t)) = \text{sign}(u_0(t))\min\{|u_0(t)|/u_m, 1 - \Delta_2\}$. The dynamic systems (2) is further written as

$$\dot{\vartheta}(t) = G_c\vartheta(t) + J_c e_T(t) + J_c\overline{\text{sat}}(u_0(t)) \tag{17}$$

where $J_c = \begin{bmatrix} 0 & 1 \end{bmatrix}^T$, $G_c = \begin{bmatrix} 0 & 1 \\ 0 & 0 \end{bmatrix}$. A function satisfying the Lyapunov conditions is constructed for the dynamic systems (2) as

$$V_c(t) = \vartheta^T(t) Q_c \vartheta(t). \tag{18}$$

According to the theorem condition (15) and the Lemma 1, the following inequality hold on:

$$\overline{\text{sat}}(u_0(t)) \le \sum_{i=1}^{2} \eta_i(\sigma_i F_c + \bar{\sigma}_i H_c)\vartheta(t). \tag{19}$$

By Theorem 1, $e_T(t)$ can converges to 0 in finite-time, the derivative of $V_e(t)$ is derived based on (19) as

$$\dot{V}_c(t) \le \vartheta^T(t)(G_c + J_c S_c)^T Q_c + Q_c(G_c + J_c S_c)\vartheta(t). \tag{20}$$

Therefore, for all $\vartheta(t) \in \Theta(Q_c, \varrho_c)$, $\dot{V}_c(t) < 0$ via condition (14) and (15), which means $\Theta(Q_c, \varrho_c)$ is a contractively invariant set. ■

Simulation studies: To verify effectiveness of the proposed yaw angle tracking control method, a simulation is carried out using Matlab software. In this simulation, initial yaw angle $\theta_d(t_k)$ is set to 60°, sampling step is 0.01 s, the total disturbances is set as $T_0 = \sin(\pi t)$, parameters on the proposed control method are adjusted as: $\gamma_v = 20$ and $\gamma_f = 0.02$ in the tracking differentiator (4), $\alpha_1 = 16$, $\alpha_2 = 8$, $\alpha_3 = 1$ and $\delta = 0.9$ in the finite-time extended-state-observer (5), $\beta_1 = -6$, $\beta_2 = -8$, $\hat{g} = 1$ and $u_m = 1$ in the tracking error feedback controller (8). Simulation results are shown in Figs. 3 and 4 under the adjusted parameters. The amphibious bionic stingray is expected to track a target by adjusting its yaw angle, therefore, the yaw angle is regulated to an origin in the simulation. As shown in the Fig. 3, the yaw angle $\theta(t)$ can smoothly approach 0°, which means that the yaw angle gradually decreases to 0° between the amphibious bionic stingray and the hypothetical target. $\bar{\theta}(t)$ is the tracking trajectory of the yaw angle $\theta(t)$, which is obtained by the tracking differentiator (4). $\hat{\theta}(t)$ is the observed values of the yaw angle $\theta(t)$, which is obtained by the finite-time extended-state-observer (5). According to the simulation results shown in the Fig. 3, both $\bar{\theta}(t)$ and $\hat{\theta}(t)$ can accurately follow the yaw angle $\theta(t)$. Similar results are shown in the Fig. 4 for the yaw angular speed $\omega(t)$ of the amphibious bionic stingray. Both $\bar{\omega}(t)$ and $\hat{\omega}(t)$ can also accurately follow the yaw angle speed $\theta(t)$. Simulation results verify the effectiveness of method proposed visual feedback disturbance rejection control method in dealing with yaw angle control for the amphibious bionic stingray under actuator saturation.

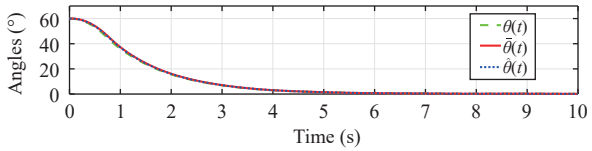

Fig. 3. Yaw angle simulation of the amphibious bionic stingray.

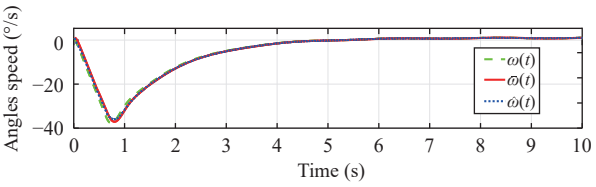

Fig. 4. Yaw angular speed simulation of the amphibious bionic stingray.

Remark 1: In this letter, limited by physical conditions of our laboratory and amphibious bionic stingray prototype, effectiveness of the proposed control method can only be verified by simulation at present. In the future, physical visual feedback control experiment will be considered to implement for the amphibious bionic stingray.

Remark 2: In this letter, a sinusoidal function is used to set as the total disturbances in the simulation. Because the total disturbances of the amphibious bionic stingray in actual motion control is complex and unknown, some functions are usually selected to represent the total disturbances in simulations for verifying the possibility of control methods such as sinusoidal function [8], [11].

Conclusion: In this letter, modeling, control method design, stability analysis and simulation verification have been carried out for an amphibious bionic stingray. The control method includes a yaw angle image recognition algorithm, a finite-time extended-state-observer and a feedback controller under actuator saturation, and its stability has been proved via Lyapunov techniques.

Acknowledgments: This work was supported by the National Natural Science Foundation of China (52175030).

References

[1] Z. Zuo, C. Liu, Q.-L. Han, and J. Song, "Unmanned aerial vehicles: Control methods and future challenges," *IEEE/CAA J. Autom. Sinica*, vol. 9, no. 4, pp. 601–614, 2022.

[2] Z. Zhou, J. Liu, and J. Yu, "A survey of underwater multi-robot systems," *IEEE/CAA J. Autom. Sinica*, vol. 9, no. 1, pp. 1–18, 2022.

[3] Z. Peng, J. Wang, D. Wang, and Q.-L. Han, "An overview of recent advances in coordinated control of multiple autonomous surface vehicles," *IEEE Trans. Ind. Informat.*, vol. 17, no. 2, pp. 732–745, 2021.

[4] J. Zhu, C. White, D. K. Wainwright, V. D. Santo, G. V. Lauder, and H. Bart-Smith, "Tuna robotics: A high-frequency experimental platform exploring the performance space of swimming fishes," *Sci. Robot.*, vol. 4, no. 34, p. eaax4615, 2019. DOI: 10.1126/scirobotics.aax4615.

[5] S. Arastehfar and C.-M. Chew, "Effects of root chord movement on thrust generation of oscillatory pectoral fins," *Bioinspir. Biomim.*, vol. 16, no. 3, p. 36009, 2021. DOI: 10.1088/1748-3190/abc86b.

[6] Q. Li, J. Zhang, J. Hong, D. Hu, Y. Yang, and S. Guo, "A novel undulatory propulsion strategy for underwater robots," *J. Bionic. Eng.*, vol. 18, pp. 812–823, 2021.

[7] Z. Peng, D. Wang, and J. Wang, "Data-driven adaptive disturbance observers for model-free trajectory tracking control of maritime autonomous surface ships," *IEEE Trans. Neural Netw. Learn. Syst.*, vol. 32, no. 12, pp. 5584–5594, 2021.

[8] J. Zhang, P. Shi, Y. Xia, and H. Yang, "Discrete-time sliding mode control with disturbance rejection," *IEEE Trans. Ind. Electron.*, vol. 66, no. 10, pp. 7967–7975, 2019.

[9] W.-H. Chen, J. Yang, L. Guo, and S. Li, "Disturbance-observer-based control and related methods−An overview," *IEEE Trans. Ind. Electron.*, vol. 63, no. 2, pp. 1083–1095, 2016.

[10] J. Han, "From PID to active disturbance rejection control," *IEEE Trans. Ind. Electron.*, vol. 56, no. 3, pp. 900–906, 2009.

[11] H. Cheng, J. Zhang, Y. Li, and J. Hong, "Finite-time tracking control for a variable stiffness pneumatic soft bionic caudal fin," *Mech. Syst. Signal Proc.*, vol. 152, p. 107314, 2021. DOI: 10.1016/j.ymssp.2020.107314.

[12] Z. Peng, Y. Jiang, and J. Wang, "Event-triggered dynamic surface control of an underactuated autonomous surface vehicle for target enclosing," *IEEE Trans. Ind. Electron.*, vol. 68, no. 4, pp. 3402–3412, 2021.

[13] J. Yu, Z. Wu, X. Yang, Y. Yang, and P. Zhang, "Underwater target tracking control of an untethered robotic fish with a camera stabilizer," *IEEE Trans. Syst. Man Cybern. -Syst.*, vol. 51, no. 10, pp. 6523–6534, 2021.

[14] Y. Yuan, Z. Wang, Y. Yu, L. Guo, and H. Yang, "Active disturbance rejection control for a pneumatic motion platform subject to actuator saturation: An extended state observer approach," *Automatica*, vol. 107, pp. 353–361, 2019.

[15] S. Yia, J. Wang, and B. Li, "Composite backstepping control with finite-time convergence," *Optik*, vol. 142, pp. 260–272, 2017.

[16] T. Hua, Z. Lin, and B. Chen, "An analysis and design method for linear systems subject to actuator saturation and disturbance," *Automatica*, vol. 38, pp. 351–359, 2002.

[17] Y. Liu, H. Li, Z. Zuo, X. Li, and R. Lu, "An overview of finite/fixed-time control and its application in engineering systems," *IEEE/CAA J. Autom. Sinica*, vol. 9, no. 5, pp. 749–762, May 2022.